JOURNAL OF MATERIALS SCIENCE 19 (1984) 1178–1184

Phase equilibria and ordering in the system HfO_2–Yb_2O_3

P. DURAN, C. PASCUAL
Instituto de Cerámica y Vidrio, CSIC Departamento de Materiales Cerámicos Especiales. Arganda del Rey, Madrid, Spain

The system HfO_2–Yb_2O_3 was investigated in the 0 to 100 mol % Yb_2O_3 range using X-ray diffraction analysis, linear thermal expansion measurements and melting point studies. At high temperatures, the system is dominated by wide regions of solid solutions based on HfO_2 and Yb_2O_3 separated by a two-phase field which appears to extend to the solidus. The extent of the cubic hafnia and ytterbia C-type solid solution fields was established using the precision lattice parameter method. At low temperature ($< 1800°$ C) two ordered phases were found in the system, one at 40 mol % ytterbia with ideal formula $Yb_4Hf_3O_{12}$, and another at ~ 70 mol % ytterbia with formula Yb_6HfO_{11}. Four eutectoid reactions and a peritectic reaction cubic ytterbia solid solution → cubic hafnia solid solution + liquid at ~ 67 mol % and ~ 2380° C have been established in the system. By incorporating the known tetragonal–cubic hafnia and C-type-hexagonal ytterbia transition temperatures, and the melting points data in the system, a tentative phase diagram is given for the system HfO_2–Yb_2O_3.

1. Introduction

Among many binary phase relations between hafnia and rare earth oxides [1, 7], the phase diagram of the system HfO_2–Yb_2O_3 is presently unknown. Perez y Jorba [8] did a detailed study of the zirconia–ytterbia system with the structural determination of solid solutions. From X-ray diffraction analysis a two-phase region was reported between 0 and 8 mol% Yb_2O_3, and only the cubic fluorite phase was present above 8 mol% ytterbia. Ordering phenomena were studied and three ordered phases were reported, phase H_1 at 40 mol % Yb_2O_3, phase H_2 at ~ 57 mol% Yb_2O_3, and H_3 at 75 mol% Yb_2O_3. Wide domains of existence were found for the two ordered phases H_1 and H_3, from 30 to 45 mol% Yb_2O_3 and from 65 to 90 mol % Yb_2O_3, respectively. This complex picture of phase transformation could not be considered as a true phase equilibrium diagram. Rouanet [9] determined the high temperature ($> 1800°$ C) phase relations and the liquidus curve for the zirconia–ytterbia system; the fluorite structure was found for 10 mol% Yb_2O_3, and the system was dominated by two wide regions of solid solution of the fluorite and C-type structures with a continuous transition between them. The transition temperature for cubic ytterbia to hexagonal Yb_2O_3 was also reported. Ordered phases were not found.

More recently, Corman and Stubican [10] have also studied the ytterbia–zirconia system, and only one ordered phase of the M_7O_{12} structure at 40 mol% Yb_2O_3 was found.

The present work was undertaken to study the tetragonal–monoclinic hafnia transformation, domains of solid solution and ordering phenomena in the ytterbia–hafnia system, using both sintered and melted samples quenched from high temperature to retain equilibrium.

2. Experimental procedure

2.1. Materials

The materials used were hafnium dioxide 99.8% and ytterbium oxide 99.9% with all others oxides of the rare earths totalling $< 0.1\%$.

2.2. Sample preparation

Weighed amounts of the starting materials were thoroughly mixed and finely ground, pressed into

0022–2461/84 $03.00 + .12

small pellets, and fired at 1300° C for several hours before further treatment. The samples were subsequently sintered at above 1800° C or melted in a solar furnace, and annealed at various temperatures below 1800° C.

Heat treatments were carried out in air using a superkanthal furnace up to 1550° C. Above 1550° C a molybdenum wound furnace with protected windings or a special gas furnace was used. A few high temperature treatments at ~ 2000° C were conducted in a flowing atmosphere (95% Ar–5% H_2) followed by cooling of the pellets as rapidly as possible.

Temperature was controlled within ± 5° C by conventional electronic controllers. Up to 1750° C the pellets were enclosed in Pt-foil and bonded with Pt-wire to the hot junction of the Pt–6Rh/Pt–30Rh thermocouple used. Above 1750° C, the temperature was measured with an optical pyrometer calibrated at the melting point of alumina. Above 2000° C the samples were held at the required temperature for long enough to establish equilibrium (no less than two hours), and then air quenched by rapid withdrawal from the furnace and allowed to cool to room temperature before being examined by X-ray diffraction. The heating times were 3 h at 2000° C, 10 h at 1800° C, 385 h at 1450° C and > 5000 h in the range 800 to 1500° C.

2.3. Thermal expansion measurements

Thermal expansion data between room temperature and 1750° C were obtained with a high temperature dilatometer, using alumina as the reference material.

2.4. Liquidus temperature measurements

The melting points of the samples containing from 40 to 70 mol% Yb_2O_3 were determined on a high-temperature thermal analysis apparatus described elsewhere [11]. The latter was calibrated at the melting points of alumina (2053° C), zirconia (2720 ± 20° C) and lanthanum oxide (2341 ± 15° C), the temperature being determined to a precision of ± 20° C.

2.5. Room temperature X-ray diffraction studies

The phases present in the quenched samples were determined at room temperature. X-ray diffraction spectrometer using Ni-filtered Cu$K\alpha$ radiation was used with a scanning speed of 2° 2θ min^{-1}. The phase boundaries of the cubic field were determined from precision lattice parameter measurements using a scanning speed of 1/4° 2θ min^{-1}. Only high angle peaks ($2\theta > 60°$) were used to calculate precise lattice parameters. A lattice parameter was calculated from each line and these data were plotted as a function of $1/2\ (\cos^2\theta/\sin\theta + \cos^2\theta/\theta)$ to obtain the correct value of the lattice parameter a_0. When only a single phase was present the precision was about ± 0.0005 nm.

3. Results and discussion

Linear thermal expansion was determined on the 1, 2, 3, 4, 5, 7, 9 and 10 mol% ytterbia compositions. Data obtained during heat up (300° C h^{-1}) of the present compositions are presented in Fig. 1. From the basis of these experiments it is clear that the monoclinic–tetragonal transformation temperature during heating is near 1590° C and remains

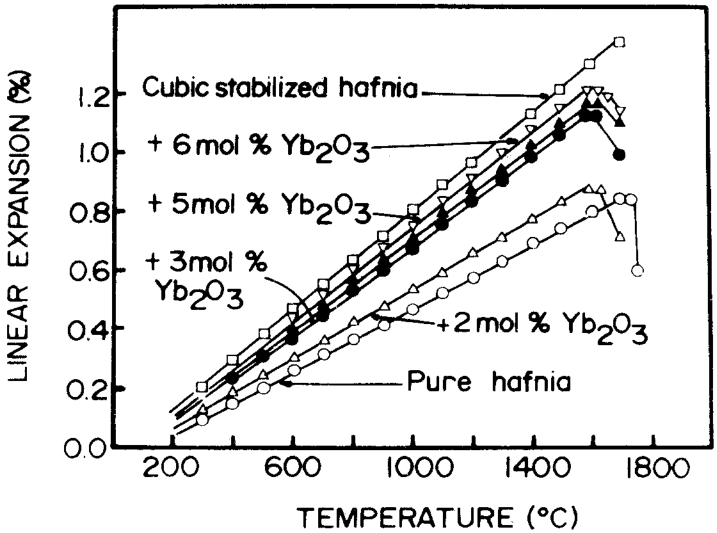

Figure 1 Linear thermal expansion for HfO_2–Yb_2O_3 compositions against temperature.

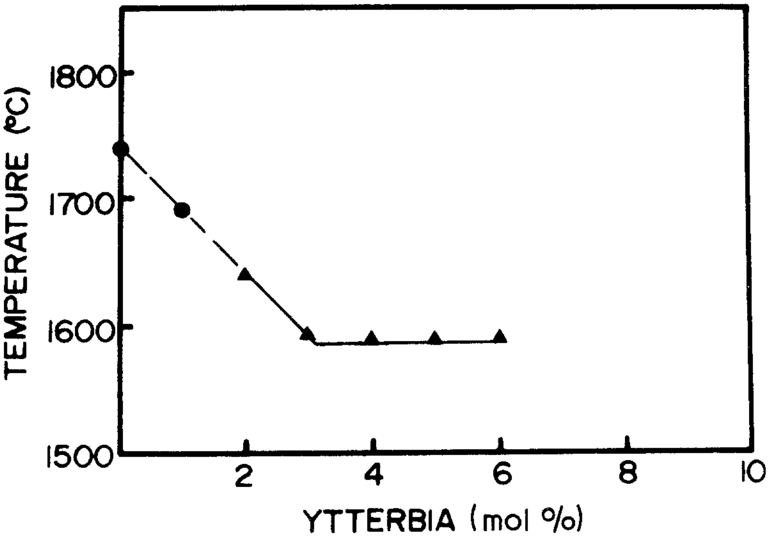

Figure 2 Effect of ytterbia on the monoclinic–tetragonal transformation temperature of hafnia.

almost constant for the 3, 4 and 5 mol% ytterbia compositions, 1630° C for the 2 mol% ytterbia and higher with decreasing content of ytterbia and for pure hafnia. Taking into account the results of Volten [12] for the monoclinic–tetragonal transformation temperature for pure hafnia, the transformation temperature value corresponding to the 1 mol% composition was extrapolated in Fig. 2. No transformation temperature was observed in the 9 and 10 mol% ytterbia compositions.

From Figs. 1 and 2 the monoclinic–tetragonal transformation temperature decreases steadily up to ~ 3 mol% ytterbia and then remains constant at ~ 1590° C. Below this temperature a two-phase region, monoclinic + cubic hafnia solid solutions, was observed between ~ 1.5 and 9 mol% ytterbia. These results lead one to the conclusion that a eutectoid reaction, tetragonal hafnia solid solution → monoclinic hafnia solid solution + cubic hafnia solid solution, takes place at about 1590° C. Above this temperature a tetragonal hafnia solid solution from 0 to about 3 mol% ytterbia appear to exist.

Below 2000° C, the phases present in the HfO_2-rich region were determined from room-temperature X-ray diffraction studies of quenched samples. The left boundary of fluorite domain was easily detected by the disappearance of the 1 1 1 and 1 1 $\bar{1}$ monoclinic hafnia solid solution peaks. This method was used to define the boundary as ~ 14 mol% ytterbia at 800° C, 12 mol% ytterbia at 1000° C, 10 mol% ytterbia at 1200° C, 9 mol% ytterbia at 1400° C, 7 mol% ytterbia at 1600° C, 6 mol% at 1700° C, 5 mol% ytterbia at 2000° C, and ~ 3.5 mol% ytterbia at 2200° C.

All samples containing more than 10 mol% ytterbia and which had been melted in the solar furnace and cooled rapidly were cubic fluorite or C-type in structure. However, when melted samples ranging from 55 to 70 mol% ytterbia were slowly solidified, the existence of a two-phase domain was particularly clear in the melted samples containing 55, 60 and 65 mol% ytterbia, and a single phase was observed for the 70 mol% ytterbia composition.

The solubility limits of ytterbia in hafnia at the right of the fluorite domain are established to be 47 mol% Yb_2O_3 at 1700° C, 50 mol% Yb_2O_3 at 2000° C and ~ 54 mol% at about 2200° C. The cubic ytterbia solid solution field extends from pure ytterbia to 33 mol% HfO_2 at about 2200° C, and 32 mol% HfO_2 at 1800° C. Fig. 3 shows the relation between lattice parameters and composition for the fluorite and C-type solid solutions.

The main goal of the present work was to establish with precision the composition and extent of the ordered phases present in this system. To do so, sintered and melted samples in the concentration range 20 to 95 mol% ytterbia were heat-treated between 700 and 1800° C. The samples were annealed for several months at 1150° C with grinding and pelleting at monthly intervals. The melted samples annealed for two or more months presented, in the range 800 to 1800° C, the following phase sequence:

$$\begin{tikzcd}
\text{Fluorite} \arrow[r, "+Yb_2O_3"] \arrow[d, shift left, "<800^\circ\,C"] & \text{Fluorite} \arrow[r, "+Yb_2O_3"] \arrow[d, shift left, "\sim1580^\circ\,C"] & \text{Fluorite}+\text{C-type} \arrow[r, "+Yb_2O_3"] \arrow[d, shift left, "\sim1680^\circ\,C"] & +\text{C-type} \arrow[d, shift left, "\sim1750^\circ\,C"] \\
\text{Mon. hafnia}+Yb_4Hf_3O_{12} \arrow[u, shift left] \arrow[r, "+Yb_2O_3"] & Yb_4Hf_3O_{12} \arrow[u, shift left] \arrow[r, "+Yb_2O_3"] & Yb_4Hf_3O_{12}+Yb_6HfO_{11} \arrow[u, shift left] \arrow[r, "+Yb_2O_3"] & Yb_6HfO_{11} \arrow[u, shift left] \\
(18\text{ mol }\%\ Yb_2O_3) & (40\text{ mol }\%) & (55\text{ mol }\%) & (70\text{ mol }\%)
\end{tikzcd}$$

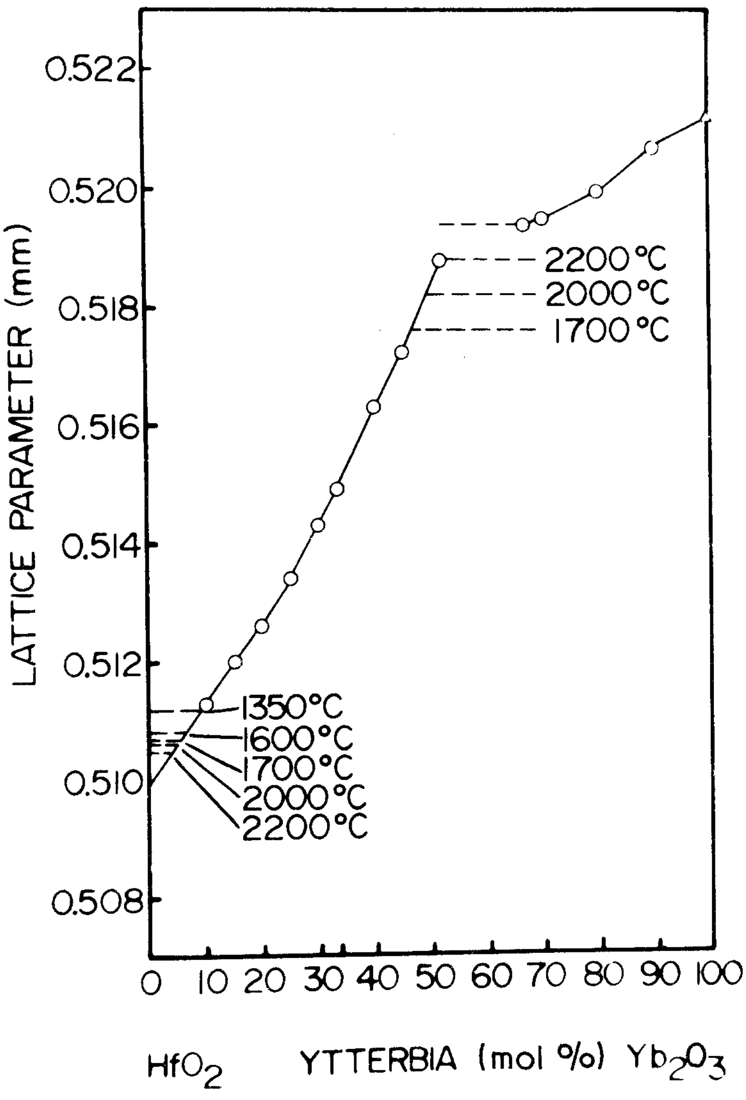

Figure 3 Room-temperature lattice parameters of HfO_2–Yb_2O_3 compositions quenched from temperatures indicates.

It should be mentioned that the δ-phase formation in this system was easier than for the others HfO_2–Ln_2O_3 systems. This fact can be related to a more favorable cationic radii Ln^{3+}/Hf^{4+} as predicted by Collonges *et al.* [13] for the δ-phase formation in similar systems ZrO_2–Ln_2O_3.

The δ-$Yb_4Hf_3O_{12}$, as for the similar δ-$Yb_4Zr_3O_{12}$ [14], may be indexed on the basis of a hexagonal unit cell. Table I shows the indexing of the δ-$Yb_4Hf_3O_{12}$. It is well known that the symmetry of these phases is rhombohedral since only $-h + k + 1 = 3n$ type reflections are present [15]. On the other hand, taking into account the studies of Bartram [16], Baezinger *et al.* [17] and Von Dreele *et al.* [18], the parameters of this ordered phase can be derived from the fluorite lattice with $a_H = a_F 7^{1/2}/2^{1/2}$ and $c_H = a_F 3^{1/2}$. Since the lattice parameter of the disordered fluorite cell (40 mol% Yb_2O_3) was $a_F = 0.5166 \pm 0.0005$ nm. From this value a_H and c_H for δ-$Yb_4Hf_3O_{12}$ were calculated to be 0.9614 ± 0.0005 and 0.8904 ± 0.0005 nm, respectively. These values are in agreement with the measured values of a_H and c_H for δ-$Yb_4Hf_3O_{12}$ as shown in Table I. The δ-phase is isostructural with UY_6O_{12}, its general formula is M_7O_{12} and its structural parameters were well defined by Bartram [16].

By heating small samples of the δ-phase to successively higher temperatures, the transition to a disordered fluorite solid solution has been found to occur at 1600 ± 25° C. At this temperature the disordering of the δ-$Yb_4Hf_3O_{12}$ phase required several hours to reach completion. At both sides of the ideal composition, the lattice parameters of

TABLE I Indexing of $Yb_4Hf_3O_{12}$ compound*

d (nm)		*hkl*	Intensity
Observed	Calculated		
0.4772	0.4808	110	M
0.3933	0.3943	012	MS
0.3755	0.3775	021	W
0.2986	0.2885	003	VS
0.2962	0.2969	211	VS
0.2767	0.2776	300	W
0.2562	0.2575	122	VS
0.2535	0.2536	113	S
0.2232	0.2236	131	M
0.2165	0.2162	104	W
0.2050	0.2052	312	M
0.2033	0.2033	303	W
0.2026	0.2028	401	MS
0.1974	0.1972	024	M
0.1866	0.1868	321	M
0.1827	0.1824	214	VS
0.1808	0.1817	410	VS
0.1756	0.1757	232	MS
0.1610	0.1607	134	M
0.1560	0.1557	125	VS
0.1553	0.1552	143	VS
0.1549	0.1550	421	VS

*Hexagonal cell; $a = 0.9614$ (30) nm, $c = 1.7908$ (30) nm.

TABLE II Indexing of Yb_6HfO_{11} compound*

d (nm)		*hkl*	Intensity
Observed	Calculated		
0.421	0.426	112	M
0.3811	0.3797	202	W
0.3028	0.3034	006	S
0.2979	0.2977	212	VS
0.2853	0.2853	106	M
0.2761	0.2753	301	W
0.2584	0.2594	214	S
0.2438	0.2455	206	MW
0.2205	0.2212	305	MW
0.2109	0.2131	224	W
0.2031	0.2036	402	M
0.1890	0.1888	226	W
0.1830	0.1846	218	VS
0.1830	0.1823	410	VS
0.1776	0.1788	412	W
0.1728	0.1720	406	W
0.1680	0.1671	500	M
0.1638	0.1637	309	M
0.1599	0.1602	331	M
0.1563	0.1563	416	VS
0.1559	0.1550	229	MS

*Hexagonal cell; $a = 0.9647$ (30) nm, $c = 1.8204$ (30) nm.

the δ-$Yb_4Hf_3O_{12}$ phase remains constant, and therefore it suggests this compound may be a phase-line in this system.

The extent of the two-phase field F_{ss} + $Yb_4Hf_3O_{12}$, and the curvature of the low ytterbia boundary of the fluorite solid solution (F_{ss}) leads one to assume that a euctectoid reaction cubic hafnia solid solution → monoclinic hafnia solid solution + $Yb_4Hf_3O_{12}$ can be present below 800° C in this zone of the system, although no conclusive experimental proofs were obtained.

Beyond 40 mol% ytterbia as the concentration increased, the intensities of the characteristic lines of δ-$Yb_4Hf_3O_{12}$ diminished and other lines appeared. These new lines, in agreement with Perez y Jorba [8], corresponds to a hexagonal phase of the M_7O_{11}-type. At ~ 60 mol% ytterbia, the intensity of the δ-phase decreased suddenly, and the lines for M_7O_{11}-type phase become more clear. This compound is similar to that found in the Er_2O_3–HfO_2 system [11], it represents a phase with the composition Yb_6HfO_{11}, and its region homogeneity extends from ~ 60 mol% to 95 mol% ytterbia. The lattice parameter measured for the hexagonal phase of the M_7O_{11}-type (70 mol% Yb_2O_3) were $a = 0.9647 \pm 0.0005$ nm and $c = 1.8204 \pm 0.0005$ nm. This phase is stable up to 1750 ± 50° C, at which temperature it decomposes into a solid solution of the C-type by an order–disorder transition. Table II shows the indexing of this hexagonal phase.

It should be mentioned that in this concentration range (from 40 to 60 mol% Yb_2O_3), another hexagonal phase of the $M_7O_{11.5}$-type was found in the system ZrO_2–Yb_2O_3 [8]. In the present work a such hexagonal phase was not found. However, taking into account that the nucleation and formation conditions of ordered phases are not well known, our failure to find the $M_7O_{11.5}$-phase does not preclude its existence.

No previous studies on the liquidus curve of the system Yb_2O_3–HfO_2 is referred to in the literature. The only references are those of Rouanet [9, 19] on the Yb_2O_3–ZrO_2 system. The more recent results of Rouanet [19] on this system show a maximum in the liquidus curve at 2825° C. A eutectic point at approximately 80 mol% Yb_2O_3 and 2420° C, which is associated with a C-type → H (hexagonal)-type phase transition in pure ytterbia near the melting point (20), was also shown. The existence of a biphasic region (F_{ss} + C-type) was not well established. In the present work it has been found that the solubility of HfO_2 in Yb_2O_3 increases with increasing temperature up to the solidus. On the other hand, the composition

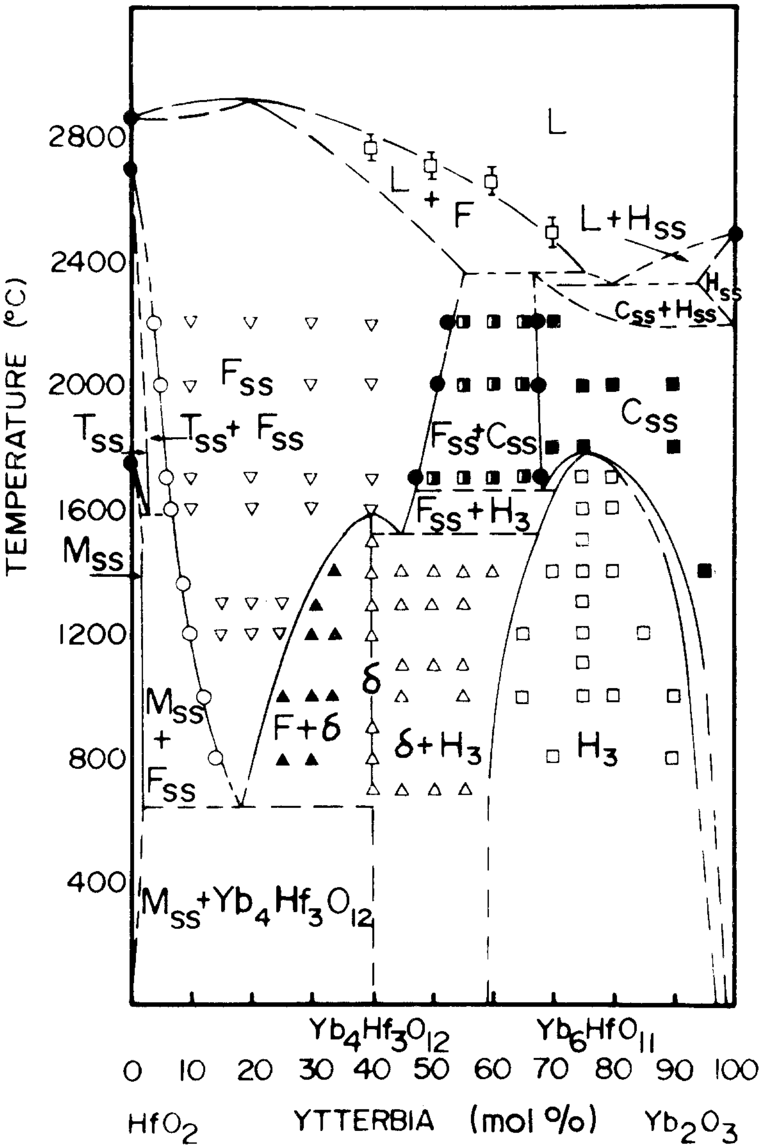

Figure 4 Phase equilibrium diagram for ytterbia–hafnia system. M_{ss}, T_{ss} and F_{ss} are monoclinic, tetragonal and fluorite hafnia solid solutions, respectively; C_{ss} = cubic ytterbia solid solution; H = hexagonal ytterbia solid solution; δ = hexagonal compound $Yb_4Hf_3O_{12}$ (40 mol% Yb_2O_3); H_3 = hexagonal compound Yb_6HfO_{11} (75 mol % Yb_2O_3).

containing 65 mol% Yb_2O_3 provides no evidence for the existence of the hexagonal-type ytterbia in the melting vicinity. This feature and the melting points determined for the compositions containing from 40 to 70 mol% Yb_2O_3 shown in Fig. 4, leads one to the assumption that a peritectic region may exist in the system at about 67 mol % Yb_2O_3 which is incorporated in the solidus.

4. Construction of the phase diagram

Based on the present data, a tentative phase diagram has been constructed in the 0 to 100 mol% Yb_2O_3 composition range (see Fig. 4). This diagram incorporates the following results:

1. The solubility of Yb_2O_3 in HfO_2 is < 1 mol % at room temperature and ~ 1.5 mol% Yb_2O_3 at 1590° C. The boundary line up to ~ 3 mol% Yb_2O_3 was traced in conformity with the results of the linear thermal expansion (see Figs. 1 and 2).
2. An extensive cubic solid solution region extends from ~ 14 mol% to 20 mol% Yb_2O_3 at 800° C and from 3.5 to 54 mol% Yb_2O_3 at ~ 2200° C. The width of this field was determined at 1000, 1200, 1400, 1600, 1700, 2000 and ~ 2200° C by using the lattice parameter method (see Fig. 3).
3. There is also a two-phase region of fluorite and cubic C-type solid solutions from 55 to 67 mol % Yb_2O_3 near the solidus, widening to 68 mol% Yb_2O_3 at ~ 1700° C.

4. A single phase solid solution of the ytterbia C-type extends from pure ytterbia to 33 mol% HfO_2 at 2200° C, and to 32 mol% HfO_2 at 1800° C.

5. Below 1800° C a long range ordering is present in the Yb_2O_3–HfO_2 system, and two hexagonal phases of the M_7O_{12} and M_7O_{11} structures at 40 and 70 mol% Yb_2O_3, respectively, were found. Both of them decompose into fluorite and C-type solid solutions, respectively, by an order–disorder process.

6. Based on the above data, five invariant points can be established for the Yb_2O_3–HfO_2 system:

(a) $$HfO_2(T_{ss}) \xrightarrow[\text{eutectoid}]{\sim 1590^\circ C} HfO_2(M_{ss}) + HfO_2(F_{ss})$$

(b) $$HfO_2(F_{ss}) \xrightarrow[\text{eutectoid}]{< 800^\circ C} HfO_2(M_{ss}) + Yb_4Hf_3O_{12}$$

(c) $$HfO_2(F_{ss}) \xrightarrow[\text{eutectoid}]{\sim 1530^\circ C} Yb_4Hf_3O_{12} + Yb_6HfO_{11}$$

(d) $$Yb_2O_3(C_{ss}) \xrightarrow[\text{eutectoid}]{\sim 1680^\circ C} HfO_2(F_{ss}) + Yb_6HfO_{11}$$

(e) $$Yb_2O_3(C_{ss}) \xrightarrow[\text{peritectic}]{\sim 2380^\circ C} HfO_2(F_{ss}) + \text{Liquid}$$

7. The phase diagram at high temperatures has been constructed to be consistent with the C-type → H (hexagonal)-type transition temperature in pure ytterbia [20], and the melting point data, thus indicating a peritectic between HfO_2 and ytterbia C-type.

Acknowledgement

The authors thank Dr J. P. Coutures of the Laboratoire des Ultrarefractaires, Odeillo, France, for the facilities given for samples preparation in the solar furnace.

This work was supported by the CAICYT, Ref. 0079/81.

References

1. L. N. KOMISSAROVA, K. S. WANG, V. I. SPITSYN and L. P. SIMANOV, *J. Inorg. Chem. (USSR)* 9 (1964) 383.
2. F. M. SPIRIDONOV, V. A. STEPANOV, L. N. KOMISSAROVA and V. I. SPITSIN, *J. Less Common Met.* **14** (1968) 435.
3. J. K. JOHNSTONE, PhD thesis, Iowa State University, Ames Iowa (1970).
4. F. M. SPIRIDONOV and L. N. KOMISSAROVA, *Zh. Neorg. Khim.* **15** (1970) 875.
5. P. DURAN, *Ceram. Int.* **1** (1975) 10.
6. V. B. GLUSHKOVA, L. V. SAZANOVA and F. GANITS, *Izv. Akad. Nauk. Neorg. Mater.* 14 (1978) 2096.
7. P. DURAN, *J. Amer. Ceram. Soc.* **62** (1979) 9.
8. M. PEREZ y JORBA, *Ann. Chim.* 7 (1962) 479.
9. A. ROUANET, *Comp. Rend. Acad. Sci. Paris* **267c** (1968) 1891.
10. G. S. CORMAN and V. S. STUBICAN, for abstract see *Amer. Ceram. Soc. Bull.* **61** (1982) 337.
11. P. DURAN, C. PASCUAL, J. P. COUTURES and S. R. SKAGGS, *J. Amer. Ceram. Soc.* **66** (1983) 101.
12. G. M. VOLTEN, *ibid.* **46** (1963) 418.
13. R. COLLONGES, F. QUEYROUX, M. PEREZ y JORBA and J. C. GILLES, *Bull. Soc. Chim. Franc.* (1965) 1141.
14. M. R. THORNBER and D. J. M. BEVAN, *J. Solid State Chem.* **15** (1975) 344.
15. V. S. STUBICAN, R. C. HINK and S. P. RAY, *J. Amer. Ceram. Soc.* **61** (1978) 17.
16. S. F. BARTRAM, *Inorg. Chem.* 5 (1966) 749.
17. N. C. BAEZINGER, H. A. EICK, H. S. SCHULDT and L. EYRING, *J. Amer. Chem. Soc.* **83** (1961) 2219.
18. R. B. VON DREELE, L. EYRING, A. L. BOWMAN and J. L. YARNELL, *Acta Crystallogr.* **B31** (1975) 971.
19. A. ROUANET, *Rev. Int. Hautes Temp. Refract.* 8 (1971) 161.
20. J. P. TRAVERSE, Thesis, CNRS A05879 (1971).

Received 13 May
and accepted 21 July 1983